Predicting Photosynthesis for Ecosystem Models

Volume I

Editors

J. D. Hesketh, Ph.D.
Crop Physiologist
Agricultural Research, Scientific and Education Administration
U.S. Department of Agriculture
University of Illinois
Urbana, Illinois

James W. Jones, Ph.D.
Associate Professor
Agricultural Engineering
University of Florida
Gainesville, Florida

CRC Press, Inc.
Boca Raton, Florida

Chapter 5

DIFFUSION RESISTANCE MODELS

J. Robert Cooke and Richard H. Rand

TABLE OF CONTENTS

I. INTRODUCTION

In this chapter we will explore the theory used to predict the gaseous exchanges between a plant and its environment. Specifically, we will concentrate upon the entry of carbon dioxide, required by the plant in the process of photosynthesis, and the loss of water vapor from the plant. The exchange of both carbon dioxide and water vapor between the plant and its environment occurs primarily through the stomatal pores.

While the CO_2 exchange is vital to the photosynthetic process, the H_2O exchange is believed by many to be neither necessary nor desirable, although they concede that the water loss possibly does produce physiologically important cooling effects (due to the latent heat of vaporization) as well as facilitating mass transport of solutes within the plant. We will not attempt to resolve this issue. Rather, we will present a formalism which can be used to predict the steady state rates of these exchanges.

Our discussion will proceed in several parts. Following a brief, general review of the resistance concept, the historical roots of the method will be presented in an abbreviated form. The literature is extensive, so we will focus only on the major contributions to the development of the theory, in contrast to experimental procedures.

The main body of the text is presented in three parts, corresponding to the major segments of the diffusion pathway encountered by CO_2 moving from the ambient atmosphere to the deep interior of the leaf. In the first section we determine the resistance in the boundary layer, in the stomatal pore, and in the substomatal cavity. In the second section the resistance of the intercellular air space is considered. This completes the pathway for water vapor. However, CO_2 continues as a dissolved solute to the sites of photosynthesis in the cell interior. Hence, in the final section, we discuss the additional resistance of the liquid phase to the diffusion of dissolved CO_2.

We shall be concerned only with steady state diffusion, a process governed by Laplace's (or, more generally, Poisson's) equation. If the transient changes are sufficiently slow to permit a steady state (i.e., a constant diffusion rate) approximation, we may invoke the resistance concept (Ohm's Law), which has been so successfully used to describe steady state electrical current.[11] In our discussion of this analog, we will emphasize the assumptions and approximations which are implicit in the resistance model of diffusion.

In the case of one-dimensional diffusion, i.e., where diffusion occurs everywhere in the same direction, the resistance model gives exact results. In the more general three-dimensional case, diffusion may proceed along curvilinear streamlines. This problem is more interesting mathematically and biologically, but is also of greater complexity. Nevertheless, the more realistic three-dimensional problem may be approximated by a one-dimensional model by determining equivalent one-dimensional resistance components. In this chapter we shall provide estimates for such resistances.

If the concentration of CO_2 or water vapor is known in the ambient atmosphere, then knowledge of these resistances will yield the resulting concentrations at locations within the leaf. Similarly, by a consideration of the overall concentration differences between the leaf interior and the ambient atmosphere, one can estimate the rate of gas exchange by diffusion. It is this property of the resistance model which is of greatest general interest to the crop physiologists and micrometeorologists. This overall resistance, if related to stomatal dimension and to stomatal action, can be used to portray the stomatal regulation of gas exchange.

Estimates of the overall resistance can be made from basic considerations of the geometry and chemistry involved in the individual segments of the diffusion pathway. Moreover, these computations can be compared with experimental measurements made in vivo.

The diffusion porometer is one such experimental instrument[18] used to characterize

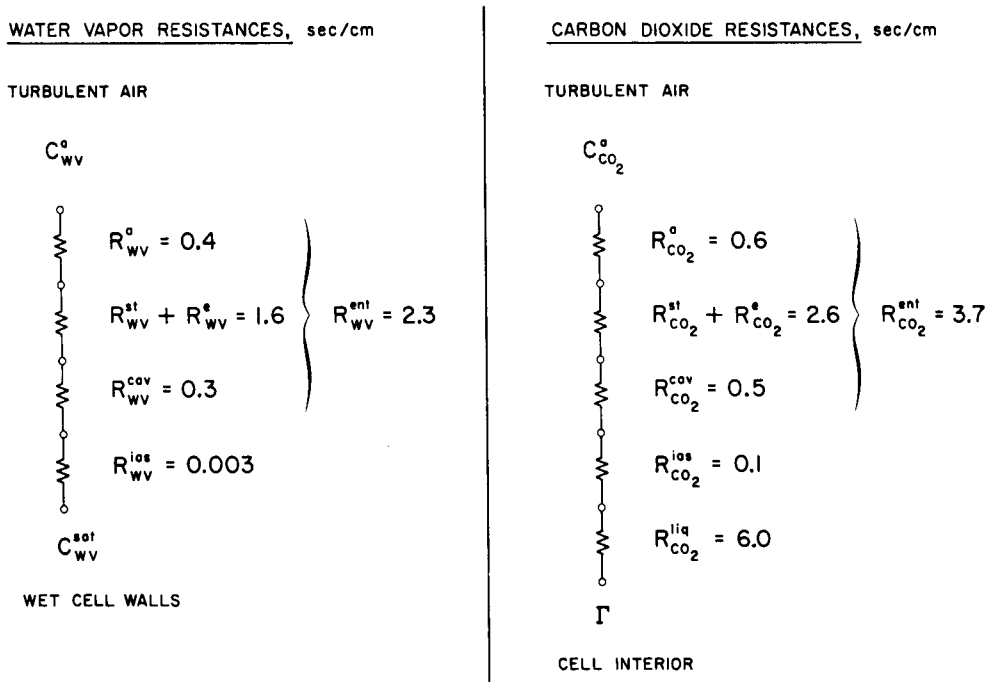

FIGURE 1. Schematic diagram of the resistances. Indicated values (in sec/cm) are to be interpreted as order-of-magnitude estimates for partially open stomates and for a typical windspeed. See text for parameters and discussion.

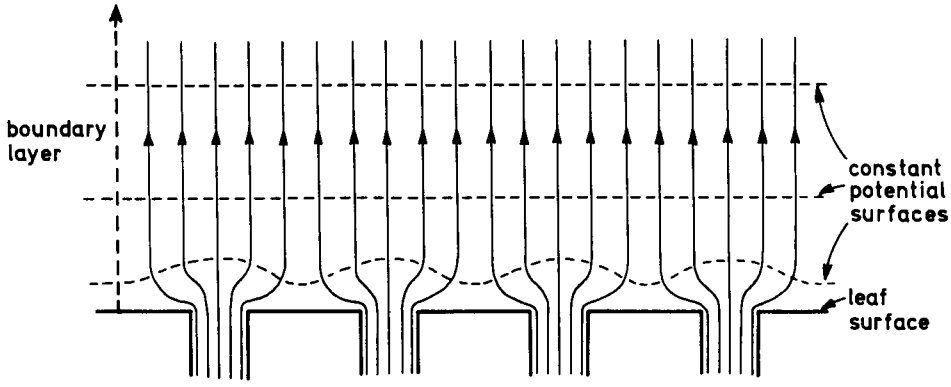

FIGURE 2. Sketch of diffusion streamlines for diffusion away from an array of stomates. From Holcomb, D. P. and Cooke, J. R., ASAE Paper No. 77-5509, American Society of Agricultural Engineers, St. Joseph, Mich., 1977.

stomatal resistance. Many different versions of the instrument have been proposed, but they have in common the measurement of a gas diffusing through actual stomates.

Figure 1 presents a schematic of the resistance model for the water vapor and carbon dioxide exchanges between the leaf and the atmosphere. This figure is central to this entire chapter. The main thrust of the following discussion is an elaboration of the correspondence of these resistances to portions of the diffusion pathway. In addition to a qualitative discussion, we also provide the equations needed for consideration of the quantitative aspects. The resistances shown in Figure 1 are presented as order of magnitude values. We will return to a discussion of these later.

The process of gaseous exchange between the leaf and the ambient environment is generally thought to occur in the manner shown in Figure 2. The gaseous exchange through the cutinized surface of the leaf is relatively small in relation to that through the stomates and will be neglected here. Diffusion of the water vapor is along the lines with arrows. The lines which intersect these flow lines at right angles are constant potential (i.e., concentration) surfaces. These constant potential surfaces become nearly flat a relatively short distance from the leaf surface. Just below the pores, but not shown in the sketch, are the substomatal cavities. We will return to a discussion of gaseous exchange after a brief literature review.

II. LITERATURE REVIEW

The resistance concept was first introduced into plant physiology in 1900 in the classic paper of Brown and Escombe.[3] They considered steady state diffusion through a plane septum with a single circular pore. By assuming that the streamlines of the flow in the pore region are exactly parallel, they uncoupled the flow in the pore from the flows outside and inside of the leaf, and so obtained an approximate expression for diffusive resistance in the gas phase. They noted in discussing the resistance to CO_2 flux that one must also include resistance due to diffusion in the liquid phase (corresponding to flow into chloroplasts inside a typical mesophyll cell), but they offered no calculation of this resistance.

Much of the literature which followed the important paper of Brown and Escombe can be interpreted as refining their model. In particular, we shall organize the literature review around the following list of criticisms of the Brown and Escombe paper:

1. The leaf exterior is modeled as an infinite region of still air and hence their model cannot account for the effects of wind. More recent investigations have discussed the dependence of the thickness of the still air layer on wind speed. See Larmor;[27] Maskell;[31] van den Honert;[62] Penman and Schofield;[46] Bange;[2] and Nobel.[39,40]
2. The Brown and Escombe model does not include a computation of the resistance of CO_2 in the liquid phase. The resistance of CO_2 diffusing as a solute has been extensively discussed. See Maskell;[31] Monteith;[37] Troughton and Slatyer;[61] Nobel;[39] Sinclair, Goudriaan, and deWit;[52] Tenhunen, Hesketh, and Gates;[57] and Sinclair and Rand.[53]
3. Since the Brown and Escombe model involves only a single pore, interactions between pores have been neglected. More recent work has revealed that this interaction effect was responsible for a significant underestimation of the overall resistance by Brown and Escombe. See Renner;[51] Maskell;[31] Verduin;[63] Monteith;[37] Ting and Loomis;[59,60] Lee;[28] Cooke;[6,7] Cook and Viskanta;[5] and Parlange and Waggoner.[45]
4. The stomatal pore cross-section is modeled by Brown and Escombe as circular, whereas it is, in fact, more nearly elliptical. The effect of noncircular pore cross-sections on stomatal resistance has been extensively considered. See Ting and Loomis;[59,60] Lee and Gates;[29] Cooke;[6] Parlange and Waggoner;[45] and Holcomb and Cooke.[19]
5. The leaf interior is unrealistically modeled in the Brown and Escombe paper as an infinite region and, therefore, their model cannot take into account morphological variations in leaf structure. More recent leaf models have included a more realistic treatment of the geometry of the leaf interior (Bange;[2] Gifford and Musgrave;[17] and Rand[49]). Stomata have been considered on upper as well as lower leaf surfaces (Waggoner;[64] Jones and Slatyer;[25] and Jones[24]), and the role of the menisci in the mesophyll cell walls (incipient drying) has been considered (Liv-

ingston and Brown;[30] Slatyer;[54] and Jarvis and Slatyer[23]). Also considered has been the influence on resistances of morphological differences due to variations in species (deWit;[13] Lee and Gates;[29] Holmgren, Jarvis, and Jarvis;[20] El-Sharkawy and Hesketh;[14] and Nobel[42]) and variations between sun and shade leaves on the same plant (Nobel, Zaragoza, and Smith;[43] Nobel;[41] and Rand[49]).

6. The resistance model approach involves an approximation which is due to the uncoupling procedure. That is, the total resistance in the Brown and Escombe paper is obtained by separately calculating the resistances outside the leaf, in the stomatal pore, and inside the leaf — and then summing these resistances. More recent works have considered the extent of the approximation which is implicit in this procedure. See Cooke;[6] Parlange and Waggoner;[45] Chapman, Cooke, and Elfving;[4] Holcomb and Cooke;[19] and Parkhurst.[44]

In addition to the above references, we wish to add the following works which have summarized the state of the art in resistance models at the time which they were written: Penman and Schofield;[46] Bange;[2] deWit;[13] Gaastra;[15,16] Kramer;[26] Milthorpe;[36] Monteith;[37] Waggoner and Zelitch;[65] Slatyer;[55] Cowan and Milthorpe;[10] Meidner and Mansfield;[34] Jarvis;[22] and Nobel.[39]

III. RESISTANCE IN THE BOUNDARY LAYER, STOMATAL PORE, AND SUBSTOMATAL CAVITY, R^{ent}

We now turn our attention to a discussion of the diffusion resistance of the region between the atmosphere and the mesophyll cell walls of the substomatal cavity. We shall assume that the gas (e.g., CO_2 or water vapor) concentration difference between these regions is known or can be estimated with reasonable accuracy. The question of estimating the diffusive flux is then just a matter of estimating the diffusive resistance. This can be done several ways.

Perhaps the most direct approach is to experimentally measure the resistance using a diffusion porometer. (See Chapman et al.[4] and Holcomb and Cooke[18] for a literature review.) Alternatively, the resistance may be predicted from a consideration of the geometric and other properties of the pathway. This latter approach will be emphasized in this discussion.

The class of papers typified by Bange[2] develops approximate resistances of portions of the pathway and then combines these to form an electrical equivalent. We shall carry these procedures to a more fundamental level. Namely, Fick's law will be assumed to govern the diffusion process, and with that as the starting point, we can estimate the order of magnitude of the discrepancy attributable to the representation of a three-dimensional problem as a one-dimensional one.[6] Two considerations are of particular interest.

First, the solution of the partial differential equation governing diffusion is known to be uniquely specified when the boundary conditions have been properly assigned. However, if the problem under consideration is arbitrarily uncoupled into several simple problems, then the resistance of the individual regions computed separately will not, in general, equal the resistance obtained by solving the partial differential equation for the original problem. This is because the uncoupling procedure involves assigning concentrations arbitrarily to surfaces internal to the boundary.

Second, the usual resistance models omit distributed sources or sinks. In situations where such considerations are important (e.g., in the intercellular air pathway and in the cell interior), we shall reexamine the fundamental models in order to obtain a more accurate understanding of the resistances involved.[44,47,53] This aspect will be developed in subsequent sections.

Steady-state gaseous diffusion under isothermal conditions in the absence of sources and sinks is governed by

$$\nabla^2 C = 0 \tag{1}$$

and

$$J_d = -D\nabla C \tag{2}$$

where C is the concentration (or diffusion potential), D the diffusion coefficient, and J_d the diffusive flux (g/cm^2sec).

An analogous set of equations for electrical current in an electrolytic solution are

$$\nabla^2 \phi = 0 \tag{3}$$

and

$$J_e = -\sigma\nabla\phi \tag{4}$$

where ϕ is the electrical potential, σ the electrical conductivity, and J_e the electrical current density. Since there is a one-to-one correspondence for the equations in the two different physical situations, a solution in one system can be related to the solution in the other.

Holcomb and Cooke[19] used this analogy to determine stomatal diffusion resistance and thereby to determine also the magnitude of the error in the widely used one-dimensional model. This analog technique permitted the study of rather complicated geometries.

If the physical phenomena are governed by the same set of equations, including the same boundary conditions, then the solution in one system can be inferred from the other. In this instance, a scale model of a typical stomatal pore can be constructed using a nonconducting material (e.g., Plexiglas®) to represent boundaries across which no diffusion occurs. Constant potential (gas concentration) boundaries can be represented by conductors.

Figure 3 depicts the geometry used by Holcomb and Cooke.[19] A circular cylinder (the boundary layer) is joined to a hemisphere (the substomatal cavity) by an elliptical cylinder (the stomatal pore).

This idealized geometry has the virtue of simplicity while retaining the essential physical aspects. In the region just external to the stomatal pore there exists a "relatively" tranquil thin layer of air known as the boundary layer. For present purposes this boundary layer (Figure 3) will be treated as a region through which gas transport away from the pore is by diffusion; that is, convection in the boundary layer will be neglected here. Beyond this idealized region, mass transport is assumed to occur by convection and will not be examined here. In Figure 2 the diffusion occurs along the curved lines, where the arrows indicate the usual direction for the diffusion of water. This region can be treated as a circular cylinder having impervious curved walls. As shown in the schematic Figure 2, the presence of adjacent pores causes the diffusion midway between pores to occur only in a direction perpendicular to the leaf, and hence is equivalent to an impervious wall. The actual shape of this cylinder need not necessarily be circular; Holcomb and Cooke[18] have shown that the spatial arrangement of the pores can depart substantially from a hexagonal pattern without destroying the usefulness of the approximation.

The elliptical cylinder for the pore is approximate because the pore length[8,50] in the

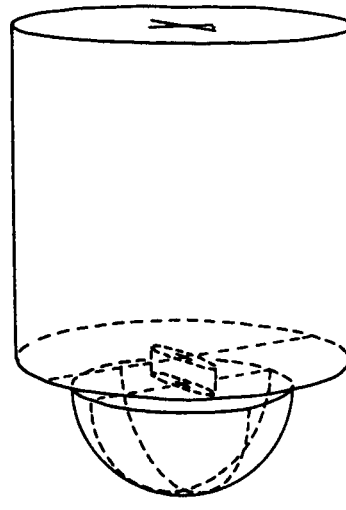

FIGURE 3. Simplified geometry assumed for a stomate. After Holcomb, D. P. and Cooke, J. R., ASAE paper No. 77-5509, American Society of Agricultural Engineers, St. Joseph, Mich., 1977.

plane of the leaf remains essentially constant during the changes in pore width, and the cross section of the pore is frequently described as being elliptical. The small gas exchange which occurs through the walls of the pore[1] is considered to be negligible in this model.

The shape of the substomatal cavity is of little importance in the computation of the resistance.[4] Consequently, the simplest shape (hemispherical) is assumed.

Holcomb and Cooke[19] developed an expression for the resistance per pore (in units of sec/cm^3) associated with Figure 3 and then converted the results to conform to the more conventional definition (with units of sec/cm).

The total resistance consisting of the sum obtained for the elliptical and circular cylinders taken separately does not equal the resistance for the two when joined together. The difference arises from the nonparallel nature of the lines of diffusion at the juncture of the two cylinders. This fundamental approximation was not treated by Bange.[2]

These resistances can be conveniently expressed in terms of the following dimensionless quantities:

1. $\alpha = (b/a) =$ the stomatal aspect ratio for the elliptical pore, i.e., the ratio of the semiminor axis, b, to the semimajor axis, a ($0.05 \leqslant \alpha \leqslant 0.5$).
2. $\beta = (r_c/a) =$ the stomatal spacing ratio, i.e., the ratio of the hypothetical radius of influence, r_c, to the semimajor axis of the elliptical pore a ($\beta \geqslant 2$).
3. $T = (\ell_c/a) =$ the nondimensional boundary layer thickness, i.e., the ratio of the dimensional boundary layer thickness ℓ_c to the semimajor axis of the elliptical pore ($T \geqslant \beta \geqslant 2$).
4. $L_P = (d/a) =$ the nondimensional pore depth, i.e., the ratio of the dimensional pore depth, d, to the semimajor axis of the elliptical pore ($L_P \geqslant 0$).

4. $L_P = (d/a) =$ the nondimensional pore depth, i.e., the ratio of the dimensional pore depth, d, to the semimajor axis of the elliptical pore ($L_P \geq 0$).

Since the parameters α, β, T, and L_P will play an extensive part in the following discussion, we will discuss the significance of typical values before proceeding.

α represents the shape of the stomatal pore as viewed from above the leaf surface. $\alpha = 1$ would correspond to a circular pore, while $\alpha = 0$ represents a "crack". The work which follows assumes that α lies in the range $0.05 \leq \alpha \leq 0.5$.

β equals the average spacing between pores, measured in semimajor elliptical pore axes a. For example, if $\beta = 2$, the pores are spaced very closely together, the centers of neighboring pores being an average of only two major pore axes (2a) apart. On the other hand, $\beta = 10$ represents pores spaced relatively far apart. A typical value for β in real leaves is about 5.[19]

Note that α/β^2 represents the fraction of leaf surface which exposes the leaf interior. With $\alpha = 0.5$ and $\beta = 5$, the stomatal pores account for about 2% of the leaf surface. Note that β is related to N, the number of stomata per unit leaf area. In fact, $N = (\pi r_c^2)^{-1}$, so that $\beta = r_c/a = (\pi N)^{-1/2}/a$.

T measures the boundary layer thickness, again in terms of semimajor pore axes. In what follows, we will view T as a given parameter. In fact, T can be related to leaf diameter and wind velocity. Nobel[39] gives

$$\ell_c \simeq 0.4 \left(\frac{L_{leaf}}{V_{wind}} \right)^{1/2} \tag{5}$$

where ℓ_c = boundary layer thickness in cm, L_{leaf} = leaf diameter in cm, and V_{wind} = wind velocity in cm/sec. A relatively thick boundary layer might correspond to ℓ_c = 0.25 cm while a relatively thin boundary layer might have ℓ_c = 0.025 cm. For a stomate with semimajor axis a = 10 μm = 10^{-3} cm, these values of ℓ_c give T = 250 (thick) and T = 25 (thin), respectively.

L_P indicates how deep the pore is, compared to the semimajor axis a. A typical value of L_P might be 1/2, although the qualitative results which follow are not very sensitive to this parameter.

The following resistance components (sec/cm) on a unit leaf area basis are given by Holcomb and Cooke[19] where the diffusion coefficient is D: the cavity resistance between mesophyll cell walls and the inner end of the pore

$$R^{cav} = (a/D)\ (\beta^2/2)\ \ln\ (4/\alpha) \tag{6}$$

the stomatal pore resistance from the inner end to the outer end

$$R^{st} = (a/D)\ L_p\ \beta^2/\alpha \tag{7}$$

the unstirred air or boundary layer resistance

$$R^a = (a/D)T \tag{8}$$

and the end effect correction

$$R^e = (a/D)\ [(\beta^2/2)\ \ln\ (4/\alpha) - \beta] \tag{9}$$

The resistance of the substomatal cavity, the stomatal pore, and the air boundary layer is the sum of the four equations, 6 to 9, provided $\beta \geq 2$, $0.05 \leq \alpha \leq 0.5$, and $T \geq \beta$, and will be called R^{ent} here to indicate entry resistance.

$$R^{ent} = (a/D)\ [T + L_p\beta^2/\alpha + \beta^2 \ln (4/\alpha) - \beta] \qquad (10)$$

The diffusion resistance, R^{ent}, for this region is seen to depend on α, β, L_p, and T and to have (a/D) as a common factor. The relative importance of these variables in determining the resistance can now be explored. In the preceding discussion, we have neglected the relatively small term for diffusion through the leaf cuticle. For a discussion of the procedure for inclusion of this effect, we refer the reader to the treatment by Nobel.[39]

Although the equations may be used in a quantitative sense, we find a qualitative discussion of the relationships informative. Rather than discuss the resistance directly, we will consider the nondimensional conductance on a unit leaf area basis $(a/D)/R^{ent}$. (Note that a/D has the units of resistance and therefore nondimensionalizes $1/R^{ent}$.) For a given concentration difference, the nondimensional conductance is simply proportional to the diffusion rate.

Figure 4 shows the nondimensional conductance for the entry region, $(a/D)/R^{ent}$, as a function of the nondimensional pore width α and the nondimensional boundary layer thickness T for two different stomatal spacings ($\beta = 5$, surface ADEJIFA; and $\beta = 10$, surface ABCHGFA) at one pore depth ($L_P = 0.5$). In all cases the conductance is zero for a closed pore ($\alpha = 0$) and increases monotonically as the pore opens (e.g., curves ABC, ADE, FGH, FIJ). For widely spaced stomates ($\beta = 10$, i.e., lower surface in Figure 4), an increase in the boundary layer thickness from $T = 25$ to 250 produces only a modest decrease in conductance (e.g., curve HC). In contrast, for more closely spaced stomates ($\beta = 5$) the same increase in boundary layer thickness produces a much larger decrease in conductance (i.e., curve JE).

The $\beta = 5$ surface illustrates one of the well-known properties of stomates. Kramer,[26] for example, states that

> It is apparent that transpiration increases rapidly with increase in aperture (AD, FI) as the stomata begin to open, but at low rates of evaporation (large T) there is little further increase in the rate of transpiration over a wide range of increase in aperture (DE). In contrast, with a high rate of evaporation (small T), the rate of transpiration increases up to the widest apertures obtained (FIJ).

Another remarkable aspect of the diffusive capacity of stomates is also apparent from Equation 10 (Kramer[26]). Although the open stomatal pores may account for perhaps only 1 or 2% of the stomate-bearing surface, the rate of water loss per unit area may be even more than half of the evaporation from an exposed water surface of the same area. The explanation usually given for this property centers on the diffusion pattern at the edges of the pore, where gradients become large as a result of the geometry. However, an equally important aspect has not been appreciated.

Figure 5 shows the fraction (R^a/R^{ent}) of the resistance R^{ent} attributable to the boundary layer. The figure has an alternative interpretation. If the same boundary layer is assumed to exist on a free-water surface as on the stomate-bearing surface, then Figure 5 is also a plot of the ratio of the diffusion rate of water through the stomates to the diffusion rate for a free-water surface. For a modest pore opening ($\alpha = 0.2$) with a typical spacing ($\beta = 5.0$), a typical pore depth ($L_p = 0.5$), and a reasonable boundary layer thickness ($T = 125$), the diffusion rate for the stomates is 49% of that for a free-water surface, as expected from the experimental literature. For a thin boundary layer ($T = 25$) the percentage is only 16%, but for a thick boundary layer ($T = 250$) this value becomes 65%. Clearly, this is an indication of the major role of the boundary layer along with the stomatal geometry and spacing in determining R^{ent}

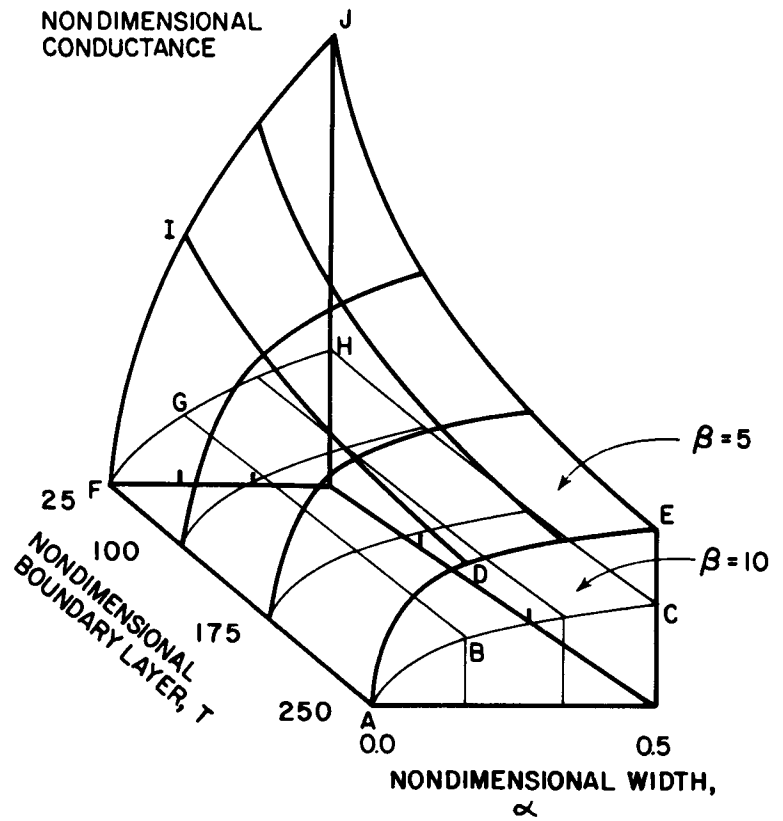

FIGURE 4. The nondimensional conductance of the entry region ($[a/D]/R^{ent}$) is shown for Equation 10 as a function of nondimensional pore width (α = b/a) and nondimensional boundary layer thickness ($T = \ell_c/a$) for two nondimensional pore spacings ($\beta = r_c/a$ = 5, 10) at one nondimensional pore depth (L_p = d/a = 0.5).

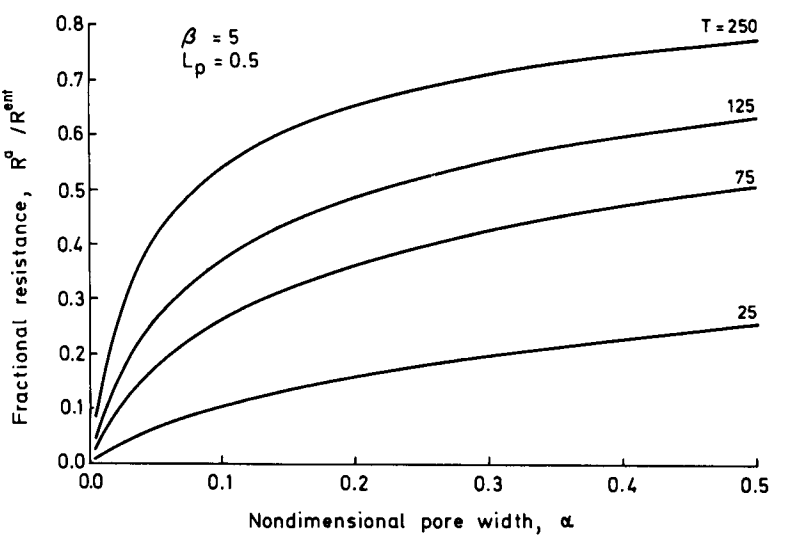

FIGURE 5. The fraction (R^a/R^{ent}) of the entry resistance R^{ent} due to the boundary layer R^a is shown as a function of nondimensional pore width (α = b/a) for several nondimensional boundary layer thicknesses ($T = \ell_c/a$) with a given nondimensional spacing ($\beta = r_c/a$ = 5) and nondimensional pore depth (L_p = d/a = 0.5).

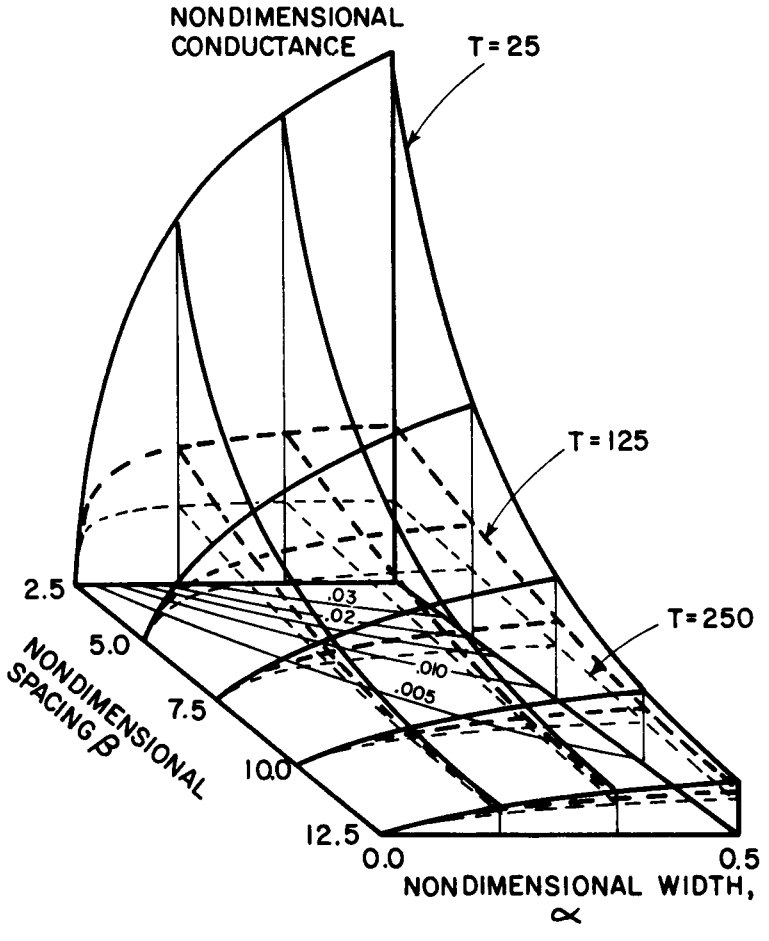

FIGURE 6. The nondimensional conductance ($[a/D]/R^{*\prime}$) is shown for Equation 10 as a function of nondimensional pore width (α = b/a) and nondimensional spacing (β = r_c/a) at selected nondimensional boundary layer thicknesses (T = ℓ_c/a). The fractional portion of the leaf surface which the pore opening constitutes is α/β^2 and is shown in the α, β plane.

This remarkable diffusive capacity has substantial biological significance. Only a relatively small fraction of the leaf interior (say < 2%) need be exposed directly to the atmosphere while still permitting sufficient carbon dioxide exchange between the leaf's interior and the atmosphere for photosynthesis to occur.

For closely spaced stomates ($\beta \leq 5$), changes in the boundary layer thickness can have a substantial effect (Figure 4) upon diffusion rate unless the control mechanism of the stomate alters the pore width. In contrast, for less dense stomates a change in air layer thickness produces a negligible direct change in conductance. Nevertheless, note that for any given boundary layer and stomate size, a decrease in spacing increases the conductance.

A different presentation of the relationships is useful. Figure 6 describes the conductance as a function of spacing and pore width at three selected air layer thicknesses (with L_p = 0.5). This figure is convenient for a discussion of the limitations of genetically altering stomatal density.

Since the nondimensional conductance explicitly includes the pore's semimajor axis in the definition, let us suppose it is to remain unchanged in the following discussion of stomatal density changes. As before, boundary layer thickness plays a less promi-

nent role in determining conductance for widely spaced stomates ($\beta = 12.5$) than for dense stomates ($\beta = 2.5$). The change between $\beta = 2.5$ and 7.5 is much greater than between 7.5 and 12.5. The relative role of the boundary layer thickness becomes quite substantial for closely spaced stomates. Furthermore, the sensitivity to changes in pore width is greatest for closely spaced stomates. In fact, for closely spaced stomates with a large boundary layer, the stomates behave somewhat like an off/on valve.

One final relationship, shown in Figure 6, will now be considered. Namely, the curves in the (α, β) plane locate α, β combinations which represent the same fraction (α/β^2) of the leaf surface which is available for gas exchange. The fractional area is less than 0.02 to 0.03. That the conductance is not simply proportional to the fractional area is obvious from Figure 6 because the projections of α/β^2 curve onto each of the surfaces at different boundary layer thicknesses do not coincide with constant conductance contours.

Finally, we compare the results of this section with those obtained by Nobel[39] (his Equation 7.5) for a circular pore of equal area. In terms of the quantities used in this paper, Nobel's equation becomes

$$(R^{ent} - R^{\bullet}) = (a/D)\ [L_p\beta^2/\alpha + \beta^2/(\alpha)^{1/2}] \qquad (11)$$

The agreement between Equation 11 and Equation 10 with T = 0 depends greatly upon the particular parameters used. For a nearly closed pore ($\alpha = 0.05$) with $\beta = 6$ and $L_P = 0.5$, Nobel's results exceed the results from this paper by only 2%. However, if the pore is opened ($\alpha = 0.5$) but the other parameters are not altered, Nobel's equation underestimates the results presented here by 18%. The difference, due to the end effect correction, can be significant.

The pore depth L_p has been held constant throughout this discussion at 0.5 because variation in a reasonable range (say $0.25 \leqslant L_P \leqslant 1.00$) does not produce an appreciable qualitative difference in the functional relationship.

The much discussed "interference effect" of stomates has been treated in a quantitative fashion here. Although the diffusion rate per stomate decreases as the pores become closer, the flux per unit leaf area increases monotonically as pore width α increases and as spacing β, boundary layer thickness T, and pore depth L_P decrease. There is no set of parameters which produce a relative maximum as a result of the interference.

In order to obtain numerical estimates for R^{ent}_{wv} and R^{ent}_{CO2}, we will take the following typical values for the parameters:

$a = 10\,\mu m = 10^{-3}$ cm
$D_{wv} = 0.25$ cm²/sec
$D_{CO_2} = 0.16$ cm²/sec
$T = 100$
$L_P = 1$
$\beta = 6$
$\alpha = 0.1$

These values, when substituted into Equation 10 give

$$R^{ent}_{wv} = 2.3 \text{ sec/cm} \qquad (12)$$

and

$$R^{ent}_{CO_2} = 3.7 \text{ sec/cm} \qquad (13)$$

IV. RESISTANCE IN THE INTERCELLULAR AIR SPACES, R^{ias}

After entering the leaf via the stomatal pore, diffusing CO_2 passes beyond the substomatal cavity and flows through the intercellular air spaces (ias) to be absorbed into the wet mesophyll cell walls. On the other hand, water vapor is free to evaporate from these walls into the ias and to then flow out of the leaf via the substomatal cavity and stomatal pore. In this section we will consider the resistances $R^{ias}_{CO_2}$ and R^{ias}_{wv} associated with these fluxes (cf. Figure 1). In particular, it will be shown that these resistances are relatively small.

If one were to model the flow in the ias by one-dimensional diffusion, then[39]

$$R^{ias}_{CO_2} = \frac{\delta^{ias}_{CO_2}}{D_{CO_2}} \tag{14a}$$

and

$$R^{ias}_{wv} = \frac{\delta^{ias}_{wv}}{D_{wv}} \tag{14b}$$

where δ denotes a representative pathway length. Note that these equations are based on analyses which neglect both the gradual absorption of CO_2 and the gradual evaporation of water vapor along the walls of the ias. In this section we will present a model which includes these effects.

Here D_{CO_2} and D_{wv} are diffusion constants in air while $\delta^{ias}_{CO_2}$ and δ^{ias}_{wv} are representative pathway lengths. The pathway lengths for H_2O and CO_2 are usually taken as about equal ($\delta^{ias}_{CO_2} = \delta^{ias}_{H_2O}$ and since (at 20°C)

$$D_{wv} = 0.25 \text{ cm}^2/\text{sec}$$

and

$$D_{CO_2} = 0.16 \text{ cm}^2/\text{sec}$$

$R^{ias}_{CO_2}$ is usually taken as 1.6 (= 0.25 /0.16) times as great as R^{ias}_{wv}.[39]

However, there has been much recent experimental evidence[1,32,33,56] which suggests that

$$\delta^{ias}_{CO_2} >> \delta^{ias}_{H_2O}$$

Consider, for example, the experiment of Aston and Jones.[1] A radioactive tracer (monosilicic acid) which moves with water and accumulates at water evaporation sites was introduced at the roots of *Avena sterilis* (Algerian oats) plants. Then X-ray microprobe analysis on freeze-substituted leaf tissue revealed that the most intensive regions of evaporation within the leaf mesophyll were the substomatal cavities. "Walls exposed to intercellular spaces, not directly connected to stomatal pores, appeared to have relatively low evaporative intensity."[1]

This effect may be predicted on theoretical grounds as the following model shows.[47,48] The model includes diffusion from the mesophyll cell walls which line the ias (corresponding to evaporation or absorption), as well as diffusion along the length of the ias.

X = 0 X = L

LEAF INTERIOR SUBSTOMATAL CAVITY

$\frac{dC_i}{dx} = 0$ $C_i = \hat{C}_i$

NO FLUX CONCENTRATION GIVEN

FIGURE 7. A simplified model of a single intercellular air space (ias).

Consider a single ias (see Figure 7) to be modeled as a circular cylinder of radius r, reaching from the deep leaf interior (x = 0) to the substomatal cavity (x = L). The mesophyll cells are assumed to be distributed uniformly around the walls of the ias.

Let $C_i(x)$ represent the concentrations (g/cm³) of water vapor (i = 1) and CO_2 (i = 2), respectively, at the center line of the ias at cross section x. That is, $C_1 = C^{ias}{}_{wv}$ and $C_2 = C^{ias}{}_{CO2}$. The boundary conditions of Figure 7 are assumed.

Evaporation of water vapor from, and absorption of CO_2 into, the walls of the ias are modeled as diffusion processes driven by the concentration difference between the centerline of the ias and the walls. In particular, we assume that the radial flux is given by

$$\text{radial flux} = \frac{D_i}{r}(C_i^* - C_i) \tag{15}$$

where $C^*_i = C^*_i(x)$ = concentration of gas i at the wall of the ias (of radius r), at cross section x. Note that C_i is taken at the centerline of the ias while C^*_i is taken at the wall.

Balancing this radial flux with the diffusive flux along the length of the ias gives[47]

$$\frac{d^2C_i}{dx^2} + \frac{2}{r^2}(C_i^* - C_i) = 0 \qquad i = 1, 2 \tag{16}$$

Both C_1 (water vapor) and C_2 (CO_2) must satisfy this differential equation with the boundary conditions of the figure; thus far the derivation is the same for both gases. When considering the quantity C^*_i, however, the two gases receive separate treatment.

Since the cell wall liquid is a dilute aqueous solution, we assume that[55]

$$C_1^* = C_1^{sat} = \text{constant}$$

where $C^{sat}{}_1$ = saturation value of C_1 in air at some assumed constant temperature. As for C^*_2, it is known that at typical leaf temperatures[39]

$$C_2^* \cong C_2^{liq}$$

where $C^{liq}{}_2 = C^{liq}{}_2(x)$ = concentration of CO_2 in cell wall liquid.

Now the flux of gaseous CO_2 from the ias into the mesophyll cell walls equals the flux of dissolved CO_2 passing through these walls into the chloroplasts. Assuming for

simplicity that the CO_2 concentration in the chloroplasts is zero,[37] the flux of dissolved CO_2 becomes $C^{liq}{}_2/R^{cell}{}_{CO2}$ where $R^{cell}{}_{CO2}$ is the resistance associated with this flux. As noted by Nobel[41-43] and Rand,[49] this resistance $R^{cell}{}_{CO2}$ refers to flux per unit cell wall area, to be contrasted with R^{liq} CO_2 discussed in the next section, which refers to flux per unit leaf area. They are related[41-43] as follows:

$$R^{cell}_{CO_2} = R^{liq}_{CO_2} \, (A^{mes}/A)$$

where A^{mes}/A is the surface area of mesophyll cells under a leaf area A.

Conservation of mass requires

$$\frac{D_2 (C_2 - C_2^*)}{r} = \frac{C_2^{liq}}{R^{cell}_{CO_2}} \tag{17}$$

Using $C^*{}_2 = C^{liq}{}_2$ (see above), one finds that

$$C_2^* = (1 + \gamma^2)^{-1} \, C_2$$

where

$$\gamma^2 = \frac{r}{D_2 R^{cell}_{CO_2}}$$

Note that r/D_2 is the resistance associated with CO_2 vapor flux from the centerline of the ias to the wall. Thus the parameter γ^2 is the ratio of two resistances encountered by diffusing CO_2. For typical values of r, D_2, and $R^{cell}{}_{CO2}$, the parameter $\gamma^2 << 1$. With $r = 5$ μm, $D_2 = 0.16$ cm^2/sec, and $R^{cell}{}_{CO2} = 100$ sec/cm (see Reference 42), we find that $\gamma = 0.0056$. The bionomial expansion then gives

$$C_2^* = (1 - \gamma^2) C_2 \qquad \gamma^2 << 1$$

Substituting the expressions $C^*{}_1$ and $C^*{}_2$ into Equation 16, we obtain

water vapor $$\frac{d^2 C_1}{dx^2} + \frac{2}{r^2} (C_1^{sat} - C_1) = 0$$

and

CO_2 $$\frac{d^2 C_2}{dx^2} + \frac{2\gamma^2}{r^2} C_2 = 0$$

These equations with the boundary conditions of Figure 7 possess the following solutions:

water vapor: $$C_1(x) = C_1^{sat} + (\hat{C}_1 - C_1^{sat}) \frac{\cosh(\lambda x/L)}{\cosh \lambda}$$

and

CO_2 $$C_2(x) = \hat{C}_2 \frac{\cosh(\gamma \lambda x/L}{\cosh(\gamma \lambda)} \tag{18}$$

where $\lambda = \sqrt{2}\,(L/r)$. With $r = 5$ μm and $L = 200$ μm (see Jarvis and Slatyer[23]), we find $\lambda = 57$.

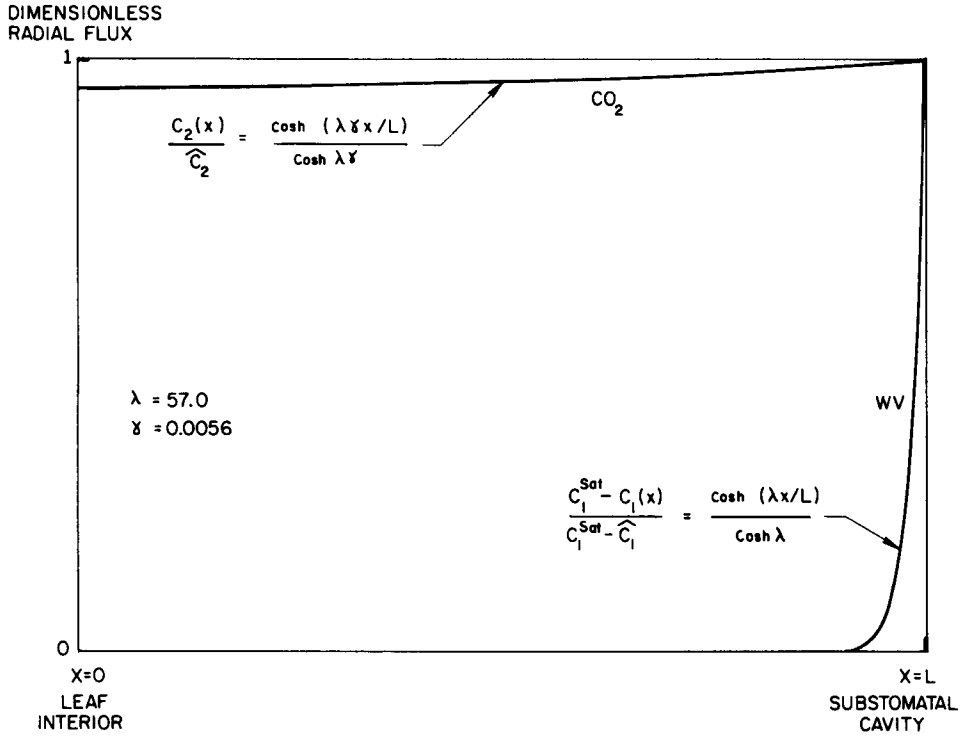

FIGURE 8. Equation 18 displayed in dimensionless form for $\lambda = (2)^{1/2}\ L/r = 57$, $\gamma = (r/[D_{CO_2} R^{cell}_{CO_2}])^{1/2} = 0.0056$. Note that most of the evaporation of water vapor is predicted to occur near the substomatal cavity end of the intercellular air space.

These equations are displayed in Figure 8 in a nondimensional form. The ordinate of Figure 8 represents the radial flux of Equation 15, normalized by dividing by the radial flux at x = L.

Figure 8 shows that the model predicts that most evaporation of water vapor occurs near the substomatal cavity end of the ias, x = L. Absorption of CO_2 into mesophyll cell walls, however, is significant all along the length of the ias. As Meidner[32] has noted, "This fits the primary function of these walls, namely to offer a moist surface for the absorption of carbon dioxide rather than for evaporation."

It should be noted that $C_2 = C^{ias}_{CO_2}$ varies with position x along the ias. Mesophyll cells far from any substomatal cavity will receive a smaller quantity of CO_2 to assimilate than cells near some substomatal cavity. However, an estimate based on a model similar to the above, but involving a more realistic leaf geometry (including two distinct regions corresponding to palisade and spongy mesophyll tissue), shows that this effect is small.[49] For example, for a 300-μm thick sun leaf, the model in Reference 49 predicts that $C^{ias}_{CO_2}$ in the deep interior of the leaf drops to only 86% of its value at the substomatal cavity.

To return to the question of resistances, if we were to interpret the predictions of this model in terms of Equations 14, we would conclude that

$$\delta^{ias}_{CO_2} >> \delta^{ias}_{wv}$$

Specifically, if one identifies δ^{ias} with the distance along the ias (measured from the substomatal cavity) which is responsible for 90% of the total flux of gas i, then[47]

$$\delta^{ias}_{wv} = 0.04L$$

and

$$\delta^{ias}_{CO_2} = 0.87L$$

That is

$$\delta^{ias}_{wv} \simeq 0.05\ \delta^{ias}_{CO_2}$$

Therefore, instead of the usual approach[39] of taking $R^{ias}_{CO_2}$ as about 1.6 times larger than R^{ias}_{wv}, we find that (Equation 14)

$$R^{ias}_{CO_2} = R^{ias}_{wv} \cdot \frac{\delta^{ias}_{CO_2}}{\delta^{ias}_{wv}} \cdot \frac{D_{wv}}{D_{CO_2}}$$

and

$$R^{ias}_{CO_2} \simeq 30\ R^{ias}_{wv}$$

For example, using $L = 200\ \mu m$,

$$\delta^{ias}_{wv} = 8\mu m$$

$$\delta^{ias}_{CO_2} = 174\ \mu m$$

$$R^{ias}_{wv} = \frac{\delta^{ias}_{wv}}{D_{wv}} = 0.003\ \text{sec/cm}$$

$$R^{ias}_{CO_2} = \frac{\delta^{ias}_{CO_2}}{D_{CO_2}} = 0.1\ \text{sec/cm}$$

As noted by Nobel,[39] these resistances are "relatively small compared with other resistances encountered by gases diffusing into or out of leaves."

We have now considered the portion of the water transport pathway through the plant in which water is the vapor phase. Therefore, the preceding discussion completes the review of the diffusion resistance of water vapor. However, carbon dioxide continues to diffuse further into the leaf interior as a dissolved gas. That portion of the CO_2 pathway will now be considered.

V. RESISTANCE OF CO_2 DIFFUSING AS A SOLUTE, $R^{liq}_{CO_2}$

After entering the leaf through the stomatal pores and diffusing through the intercellular air spaces, CO_2 is absorbed into the walls of the mesophyll cells. Continuing its journey as a diffusing solute, CO_2 then diffuses through the cellular liquid into the chloroplasts where it is utilized in the biochemistry of photosynthesis. The treatment of this process is complicated by the creation of CO_2 within the cell through respiration

and (in C-3 plants) through photorespiration. In this section we will consider the resistance $R^{liq}_{CO_2}$ associated with the diffusion of CO_2 as a solute in the cellular liquid. Note that no comparable resistance exists for water vapor.

The flow of CO_2 as a solute is driven by a concentration difference from the intercellular air space to the cell interior. This relationship is often written in the form[42]

$$J_{CO_2} = \frac{C^{ias}_{CO_2} - C^{cell}_{CO_2}}{R^{liq}_{CO_2}} \tag{19}$$

where

$C^{ias}_{CO_2}$ = CO_2 concentration in ias near cell wall

$C^{cell}_{CO_2}$ = CO_2 concentration in cell interior

J_{CO_2} = CO_2 flux taken per unit leaf area

The difficulty with this approach lies in identifying $C^{cell}_{CO_2}$: Is it the concentration in the chloroplasts, the mitochondria, or the cytoplasm? Is it an average value taken over the relevant regions of the cell? Or is it a value at some fixed position inside the cell?

The above questions are related as follows to the concept of the CO_2 compensation concentration Γ.[42,52] Γ is defined as the concentration of CO_2 at which $J_{CO_2} = 0$, i.e., the value of $C^{ias}_{CO_2}$ at which CO_2 consumption by photosynthesis is exactly balanced by CO_2 evolution due to respiration and photorespiration. Comparison of this definition with Equation 19 suggests that a more appropriate model for this flux would be

$$J_{CO_2} = \frac{C^{ias}_{CO_2} - \Gamma}{R^{liq}_{CO_2}} \tag{20}$$

Now if $C^{ias}_{CO_2} = \Gamma$, then Equation 20 automatically gives $J_{CO_2} = 0$ in agreement with the definition of Γ.

In fact this form of Fick's law was the outcome of a recent theoretical model by Sinclair, Goudriaan and deWit.[52] Since the model provides an explicit expression for $R^{liq}_{CO_2}$ in terms of basic biochemical parameters and leaf and cell geometry, we will review it here.

Sinclair et al.[52] consider a spherical cell in which the chloroplasts, mitochondria, etc. are uniformly distributed between the tonoplast and the cell surface. The boundary conditions of Figure 9 are assumed. At the tonoplast, $r = r_1$, there is no flux $dC/dr = 0$. At the cell surface, $r = r_2$, the concentration of CO_2 is given: $C = C^{ias}_{CO_2}$.

Let $C = C(r)$ be the concentration of CO_2 in the cell at radius r. The diffusion problem may then be formulated as follows:

$$\frac{D^*_{CO_2}}{r^2} \frac{d}{dr}\left(r^2 \frac{dC}{dr}\right) = \Phi_{chl} - \Phi_{pr} - \Phi_{dr} \tag{21}$$

where

$$\Phi_{chl} = \frac{V_c K_o C}{K_c K_o + K_o C + K_c O} = \text{chloroplast carboxylation rate}$$

$$\Phi_{pr} = \frac{t\, V_o K_c O}{K_c K_o + K_o C + K_c O} = \text{photorespiration rate}$$

$$\Phi_{dr} = \text{constant} = \text{dark respiration rate}$$

Here V_c = maximum enzymatic velocity for carboxylase reaction ($g/cm^3/sec$)
V_o = maximum enzymatic velocity for oxygenase reaction ($g/cm^3/sec$)
K_c = Michaelis-Menten constant for CO_2 (g/cm^3)
K_o = Michaelis-Menten constant for O_2 (g/cm^3)
O = O_2 concentration (g/cm^3)
t = fraction of CO_2 evolved in photorespiration per O_2 consumed
$D^*_{CO_2}$ = diffusion constant for CO_2 in cytoplasm

In other words, Equation 21 states that the rate of radial diffusion of CO_2 into the cell is balanced by the rate at which CO_2 is locally consumed and evolved by photosynthesis and respiration, respectively. The expressions for the carboxylation and photorespiration rates involve the usual Michaelis-Menten models.[57,58]

For C-4 plants, photorespiration is absent from Equation 21. In this case we will take $K_o \to \infty$ so that $\Phi_{pr} \to 0$.

Equation 21 is a second-order, nonlinear, ordinary differential equation for which no exact solution is known. Sinclair, Goudriaan, and deWit[52] obtained an approximate solution valid for small CO_2 concentrations, while Sinclair and Rand [53] obtained an approximate solution valid for large CO_2 concentrations. In what follows, we shall restrict ourselves to small CO_2 concentrations, and we shall follow the treatment of Sinclair, Goudriaan, and deWit.[52]

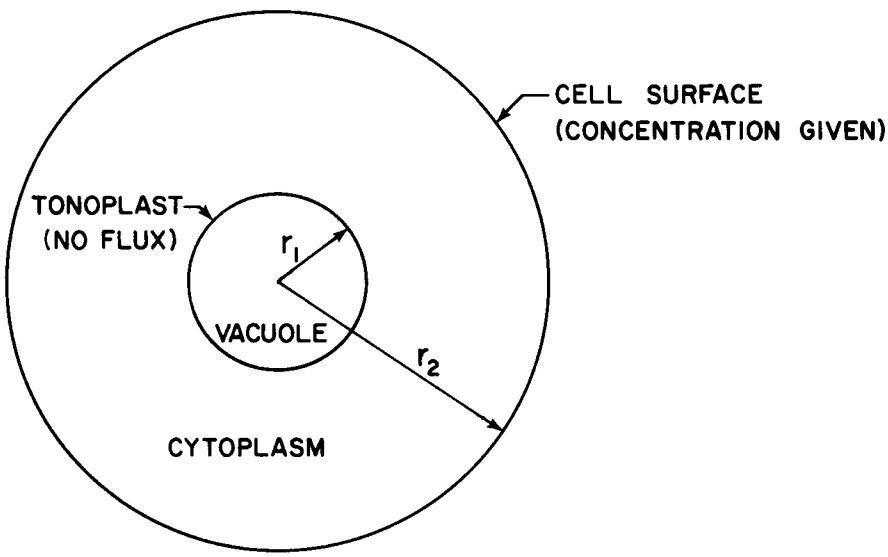

FIGURE 9. An idealized spherical cell. Boundary conditions: at the tonoplast, $r = r_1$ there is no flux, $dC/dr = 0$; at the cell surface, $r = r_2$ the concentration of CO_2 is given, $C = C^{ms}_{CO_2}$. After Sinclair, T. R., Goudriaan, J., and deWit, C. T., *Photosynthetica*, 11, 56, 1977.

For small CO_2 concentrations, Equation 21 may be linearized in C by expanding Φ_{chl} and Φ_{pr} about C = 0 and neglecting nonlinear terms. This gives

$$\frac{D^*_{CO_2}}{r^2}\frac{d}{dr}\left(r^2\frac{dC}{dr}\right) - \frac{V_c' K_o C}{K_c(K_o + O)} = -\Phi_{dr} - \frac{tV_o O}{K_o + O} \tag{22}$$

where

$$V_c' = V_c + \frac{tV_o O}{K_o + O}$$

In comparing Equation 22 with the corresponding Equation 9 of Sinclair et al.,[52] note that they have neglected the difference between V'_c and V_c.

Note that Γ, the CO_2 compensation concentration, will correspond to the value of C for which there is no flux, i.e., for which dC/dr = 0. We find from Equation 22 that

$$\Gamma = \frac{K_c}{V_c' K_o}[(K_o + O)\,\Phi_{dr} + tV_o O] \tag{23}$$

The solution to Equation 22 with the boundary conditions of Figure 9 involves hyperbolic sines and cosines and has been given by Sinclair, Goudriaan and deWit.[52] From this solution, they derive an expression for $J^{cell}_{CO_2}$, the CO_2 flux into a single spherical cell (taken per unit cell wall surface area)

$$J^{cell}_{CO_2} = D^*_{CO_2}\left.\frac{dC}{dr}\right|_{r = r_2} \tag{24}$$

which becomes

$$J^{cell}_{CO_2} = \frac{C^{ias}_{CO_2} - \Gamma}{R^{cell}_{CO_2}} \tag{25}$$

where

$$R^{cell}_{CO_2} = \frac{1}{\nu D^*_{CO_2} G} \tag{26}$$

and

$$\nu^2 = \frac{V_c' K_o}{D^*_{CO_2} K_c(K_o + O)} \tag{27}$$

and

$$G \simeq \nu r_2/3 \tag{28}$$

The nondimensional geometrical factor G always lies between zero and unity. Equation 28 for G is an approximation offered by Sinclair et al.[52] in place of the more

complicated exact expression for G given in their paper. For typical parameters,[52] they found Equation 28 to be satisfactory (although it does assume nonvacuolated cells, $r_1 = 0$). With this expression for G, the expression (Equation 26) for $R^{cell}_{CO_2}$ simplifies to

$$R^{cell}_{CO_2} = \frac{3K_c(K_O + O)}{r_2 V'_c K_O} \tag{29}$$

As in the section on resistance in the ias, let A^{mes}/A represent the surface area of mesophyll cells under leaf area A. Then[41-43,52]

$$R^{liq}_{CO_2} = \frac{R^{cell}_{CO_2}}{A^{mes}/A} \tag{30}$$

Equations 29 and 30 furnish the desired expression for R^{liq}_{CO2} of Equation 20 in terms of basic biochemical and geometrical parameters.

In order to obtain a numerical estimate for R^{liq}_{CO2}, we need values for the parameters K_c, K_o, V'_c, O, r_2, and A^{mes}/A. Following Sinclair et al.,[52] we will assume

$$K_c = \begin{cases} 7 \times 10^{-7}\ g/cm^3 & \text{C-3 plants} \\ 3 \times 10^{-7}\ g/cm^3 & \text{C-4 plants} \end{cases}$$

$$V'_c = \begin{cases} 3 \times 10^{-5}\ g/cm^3/sec & \text{C-3 plants} \\ 6 \times 10^{-5}\ g/cm^3/sec & \text{C-4 plants} \end{cases}$$

$$r_2 = 5\ \mu m = 0.5 \times 10^{-3}\ cm$$

$$A^{mes}/A = 40$$

$$\frac{K_O + O}{K_O} = \begin{cases} 1.7 \text{ for C-3 plants (20\% oxygen level)} \\ 1 \text{ for C-4 plants (no photorespiration)} \end{cases}$$

Substituting these values into Equations 29 and 30, we find

$$R^{liq}_{CO_2} = \begin{cases} 6\ sec/cm & \text{C-3 plants} \\ 0.8\ sec/cm & \text{C-4 plants} \end{cases} \tag{31}$$

In order to apply Equation 20 we also require the value of Γ. From Equation 23 Γ involves Φ_{dr}, t, and V_o, as well as K_c, V'_c, K_o, and O. We shall assume that $\Phi_{dr} = 0.03$ V'_c, $t = 0.25$, and $V_o = 0.5\ V'_c$.

Substituting into Equation 6, we find that

$$\Gamma = \begin{cases} 9.7 \times 10^{-8}\ g/cm^3 \text{ for C-3 plants} \\ 9 \times 10^{-9}\ g/cm^3 \text{ for C-4 plants} \end{cases} \tag{32}$$

It is to be emphasized that these evaluations for $R^{liq}_{CO_2}$ and Γ are based on tentative values of the biochemical parameters and are meant to offer order-of-magnitude approximations rather than statistical estimates.

Finally, we wish to compare the expression for the resistance $R^{liq}_{CO_2}$ given by Equations 29 and 30 with the more usual approach in which $R^{liq}_{CO_2}$ is taken as a series of resistances, each of the form δ/D where δ is a distance diffused and D is a diffusion constant.[39]

In particular, note that Equations 29 and 30 for $R^{liq}_{CO_2}$ do not contain a diffusion constant! This differs in a basic manner from the usual expression for $R^{liq}_{CO_2}$. The following explanation, based on two simplified one-dimensional diffusion equations, illustrates the essential distinction between the two expressions for $R^{liq}_{CO_2}$.

Problem A Diffusion without sources or sinks	Problem B Diffusion with uniformly distributed sink
$D\frac{d^2C}{dx^2} = 0$	$D\frac{d^2C}{dx^2} = \Phi = \text{constant}$
Boundary Conditions:	Boundary Conditions:
$x = 0 \quad , \quad C = C_o$	$x = 0 \qquad \frac{dC}{dx} = 0$
$X = L \quad , \quad C = C_L$	$x = L \qquad C = C_L$
Solution:	Solution:
$C = C_o + (C_L - C_o)\frac{x}{L}$	$C = \frac{\Phi}{2D}(x^2 - L^2) + C_L$
Flux:	Flux:
$J = -D\left.\frac{dC}{dx}\right\|_{x=L} = \frac{-D(C_L - C_o)}{L}$	$J = -D\left.\frac{dC}{dx}\right\|_{x=L} = -\Phi L$

Problem A could model diffusion without sources or sinks as in the stomatal pore. Problem B could model diffusion with a uniformly distributed sink as in the cell interior. Although Problem B is considerably simpler than the model of Sinclair et al.,[52] both share the property that J is independent of diffusion constant (cf. Equations 20, 29, 30). In Problem A, however, J is proportional to D.

A study of these two sample problems shows that they offer different predictions regarding the influence of diffusion constant D on flux J. Since the actual sites of photosynthesis and respiration are distributed throughout the cell, a "Problem B" format is more appropriate for modeling CO_2 flux in the cell interior (except that a more realistic three-dimensional geometry is desirable as in the Sinclair et al.[52] model). Thus we cannot expect the expression for $R^{liq}_{CO_2}$ to be of the form δ/D!

The electrical resistance analogy of Brown and Escombe[3] is suitable for application to problems of diffusion without distributed sources or sinks (as in their own original model). However, more recent attempts have been made to model diffusion in the cell interior by a "Problem A" format. We feel that the approach of Sinclair et al.[52] provides an improved model of this situation.

VI. FLUXES OF WATER VAPOR AND CO_2

On the basis of the above models, the fluxes J_{wv} and J_{CO_2} may be computed as follows (refer to Figure 1): for water vapor

$$J_{wv} = \frac{C_{wv}^{sat} - C_{wv}^{a}}{R_{wv}^{ent} + R_{wv}^{ias}}$$

Assuming

$C_{wv}^{sat} = 23 \times 10^{-6}$ g/cm³ (based on a leaf temperature of 25°C and a relative humidity of 100%)

$C_{wv}^{a} = 8.7 \times 10^{-6}$ g/cm³ (based on an ambient atmosphere temperature of 20°C and a relative humidity of 50%)

$R_{wv}^{ent} = 2.3$ sec/cm (cf. Equation 12)

$R_{wv}^{ias} = 0.003$ sec/cm (negligible)

we obtain

$$J_{wv} = 6.2 \times 10^{-6} \text{ g/cm}^2 \text{ -sec}$$

For CO_2

$$J_{CO_2} = \frac{C_{CO_2}^{a} - \Gamma}{R_{CO_2}^{ent} + R_{CO_2}^{ias} + R_{CO_2}^{liq}}$$

Assuming

$C_{CO_2}^{a} = 320$ ppm $= 57.8 \times 10^{-8}$ g/cm³

$\Gamma = 9.7 \times 10^{-8}$ g/cm³ (for C-3 plants)

$R_{CO2}^{ent} = 3.7$ sec/cm (cf. Equation 13)

$R_{CO_2}^{ias} = 0.1$ sec/cm

$R_{CO_2}^{liq} = 6.0$ sec/cm (for C-3 plants)

we obtain

$$J_{CO_2} = 4.9 \times 10^{-8} \text{ g/cm}^2\text{sec}$$

These values for J_{wv} and J_{CO_2} are in agreement with typical values given in the literature.[39]

VII. RELATED RESEARCH

In the previous sections we described the diffusion resistance in relation to the geometrical properties of the stomate and its related physiological structure. Specifically, we have assumed the stomatal dimensions to be known and to not vary with time. Stomatal movement, of course, plays a crucial role in the regulation of gaseous exchange between the plant and the environment. Quite naturally, then, the fundamental mechanical considerations which govern the static stomatal pore width are of interest, as are the factors which govern the time-dependent behavior of the pore width. If the transient motion of the pore is sufficiently slow, the steady state assumption implicit in the resistance models will still be appropriate.

For more than a century, various theories of stomatal mechanics have been explored.[50] Recently Cooke et al.[8] examined the mechanical deformations of a thin elliptical-torus model of a pair of guard cells. Since the guard cell wall adjacent to the pore is usually thicker than the wall between the guard cell and the adjacent subsidiary cell, this property was at one time thought to be the mechanical basis for pore opening. More recently the role of the radially oriented cellulose microfibrils (called micellae) has been appreciated. This radial stiffening has been shown to facilitate the opening of the pore. In Reference 8, the crucial role played by guard cell geometry has been explored in detail. An elliptical guard cell pair could open with an increase in internal hydrostatic or turgor pressure even in the absence of micellae, i.e., geometry plays a crucial role. For example, unlike stomata, a circular torus such as an automotive inner tube has a decreasing pore diameter upon inflation. When the circular cross section (top view) of the torus becomes elliptical, the pore width increases with an increase in internal pressure and decreases with an increase of pressure in the adjacent subsidiary cells. The opposing behavior of guard cells and subsidiary cells assures control of pore width without sole reliance upon an elastic restoring force to close the pore. The relative antagonism of the two competing pressures can be characterized by defining an antagonism ratio as the negative of the ratio of the change in pore width due to a unit change in internal pressure in relation to the change in pore width due to a unit change in external pressure.

A simple multilinear relationship

$$W = b_o + b_g P_g + b_s P_s \tag{33}$$

relates the pore width W to internal guard cell pressure P_g and external subsidiary cell pressure P_s, provided $W \geq 0$. The combinations of P_g and P_s which produce $W < 0$ correspond to a closed pore under conditions known as the stress phase. Within the stress phase P_g can increase without any change in pore width becoming apparent. The coefficient b_g is positive but b_s is negative. This relationship adequately reflects the experimental literature.

Equation 33 is believed to be useful over a rather wide range of pressures, although a nonlinearity is predicted for large pore widths (Cooke et al.[9]). When geometric nonlinearities are included in the analysis, the range of usefulness of Equation 33 becomes clearer. As would be expected, the pore width does not become arbitrarily large as the internal pressure is increased. Rather, the pore width gradually becomes less sensitive to pressure. Eventually an increase in pressure causes an increase in the guard cell cross section but results in a smaller pore width.

Throughout this chapter we have taken the semimajor axis of the pore to be constant. This property is evident in the experimental literature and is also predicted in the finite-element shell model.[8,9]

Stomatal action is generally considered to be based upon changes in the osmotic potential within the guard cell. Delwiche and Cooke[12] have presented an analytical model of the hydraulic aspects of stomatal dynamics in which the transient interaction of the guard and subsidiary cells is examined.

The actual scenario of stomatal opening was found to depend more heavily upon this interaction with the subsidiary cells than had been acknowledged in the physiological literature. Let us suppose that (by whatever biochemical means) the hydrostatic pressure P_g in a closed guard-cell pair begins to increase. No motion will be apparent at first if the guard cell is in the "stress phase." When the pore opens, transpiration begins and the cell wall water potential drops. This then causes the subsidiary cell pressure P_s to drop, thereby increasing further the pore opening, as is clear from Equation 33. The increase in P_g has triggered the pore opening. Since the magnitude of b_s is larger than the magnitude of b_g, the decrease in P_s becomes the major contributor in determining pore size. (This latter condition can be expressed more succinctly by saying that the antagonism ratio is greater than 1. A value of 1.5 is representative.)

The model of stomatal dynamics also provides an explanation of the stable, hydraulically based oscillations in stomatal aperture which can occur even in the absence of a periodic forcing term. The period of oscillation was shown to be strongly influenced by the cell wall conductivity.[12]

VIII. SUMMARY

The widely used electrical resistance analog for gaseous exchange by diffusion between the leaf interior and the atmosphere has been described. Some recent refinements in the application of the concept were reviewed.

The results obtained from an electrolytic tank analog in three dimensions were used to develop expressions for the "entrance resistance" which includes the boundary layer, stomatal pore, and substomatal cavity regions. The effect of the elliptical pore shape as well as the "mutual interference" of pores was treated quantitatively.

The resistance in the intercellular air spaces (ias) was shown to be relatively small. Here the model included gradual absorption of CO_2 and evaporation of water vapor along the length of an ias.

The resistance of CO_2 diffusing as a dissolved solute in the cell liquid was analyzed using a spherical cell model. In particular, this resistance was shown to depend upon geometrical and biochemical parameters, but to be approximately independent of the diffusion constant.

Finally, numerical estimates for these resistances were shown to predict fluxes of CO_2 and water vapor which are in order-of-magnitude agreement with typical values experimentally obtained by other investigators.

IX. SYMBOLS

a	Semimajor axis of elliptical pore.
A^{mes}/A	Surface area of mesophyll cells under a leaf area A.
b	Semiminor axis of elliptical pore.
b_o, b_g, b_s	Coefficients of Equation 33.
C	Concentration (g/cm^3).
C	Concentration at substomatal cavity, Figure 7.
C*	Concentration at wall of ias.
C_1	C^{ias}_{wv} = concentration of water vapor in ias.
C_2	C^{ias}_{CO2} = concentration of CO_2 in ias.
C^a	Concentration in ambient atmosphere.

C^{liq}_2	Concentration of CO_2 in cell wall liquid.
C^{sat}_1	Saturation concentration of water vapor in air at assumed temperature.
d	Stomatal pore depth.
D	Diffusion constant in air (cm^2/sec).
$D^*_{CO_2}$	Diffusion constant of CO_2 in cytoplasm.
G	Parameter of Equation 28.
J	Diffusive flux ($g/cm^2/sec$).
K_c, K_o	Michaelis-Menten constants, Equation 21.
L	Length of an ias, Figure 7.
ℓ_c	Boundary layer thickness.
L_P	d/a.
N	Number of stomata per unit leaf area.
O	O_2 concentration, Equation 21.
P_g, P_s	Turgor pressures, Equation 33.
r	Radius of a cylindrical ias, Figure 7; also distance from the center of a spherical cell, Equation 21.
r_1	Tonoplast radius, Figure 9.
r_2	Spherical cell radius, Figure 9.
r_c	$(\pi N)^{-1/2}$.
R^a	Air boundary layer resistance, Equation 8.
R^{cav}	Cavity resistance, Equation 6.
$R^{cell}_{CO_2}$	Resistance to CO_2 flux per unit mesophyll cell wall area, Equation 30.
R^e	End-effect correction resistance, Equation 9.
R^{ent}	Entry resistance, Equation 10.
R^{ias}	Intercellular air space resistance, Equation 14.
$R^{liq}_{CO_2}$	Resistance to CO_2 flux per unit leaf area, Equation 30.
R^{st}	Stomatal pore resistance, Equation 7.
t	Fraction of CO_2 evolved per O_2, Equation 21.
T	ℓ_c/a.
V_c, V_o	Maximum enzymatic velocities, Equation 21.
W	Stomatal pore width, Equation 33.
x	Distance along the length of an ias, Figure 7.
α	b/a
β	r_c/a.
γ	$[r/(D_{CO2}\, R^{cell}_{CO2})]^{1/2}$.
Γ	CO_2 compensation concentration, Equation 23.
δ^{ias}	Effective length of an ias.
λ	$\sqrt{2}\, L/r$.
ν	Parameter of Equation 27.
σ	Electrical conductivity, Equation 4.
Φ_{chl}	Chloroplast carboxylation rate.
Φ_{dr}	Dark respiration rate.
Φ_{pr}	Photorespiration rate.
ϕ	Electrical potential, Equation 4.

ACKNOWLEDGMENT

The authors wish to thank Professor T. R. Sinclair and Mr. Richard Stroshine of Cornell University for valuable discussions.

REFERENCES

1. **Aston, J. J. and Jones, M. M.,** A study of the transpiration surfaces of *Avena sterilis* L. var Algerian leaves using monosilicic acid as a tracer for water movement, *Planta (Berl.)*, 130, 121, 1976.
2. **Bange, G. G. J.,** On the quantitative explanation of stomatal transpiration, *Acta Bot. Neerl.*, 2(3), 255, 1953.
3. **Brown, H. T. and Escombe, F.,** Static diffusion of gases and liquids in relation to the assimilation of carbon and translocation in plants, *Philos. Trans. R. Soc. London Ser. B.*, 193, 233, 1900.
4. **Chapman, D. C., Cooke, J. R., and Elfving, D. C.,** A finite difference analysis of the diffusion porometer, ASAE Paper No. 77-5508, American Society of Agricultural Engineers, St. Joseph, Mich., 1977.
5. **Cook, G. D. and Viskanta, R.,** Mutual diffusional interference between adjacent stomata on a leaf, *Plant Physiol.*, 43, 1017, 1968.
6. **Cooke, J. R.,** Some theoretical considerations in stomatal diffusion: a field theory approach, *Acta Biotheor.*, 17(3), 95, 1967.
7. **Cooke, J. R.,** The influence of stomatal spacing upon diffusion rate, ASAE Paper No. 69-525, American Society of Agricultural Engineers, St. Joseph, Mich., 1969.
8. **Cooke, J. R., DeBaerdemaeker, J. G., Rand, R. H., and Mang H. A.,** A finite element shell analysis of guard cell deformations, *Trans. ASAE*, 19(6), 1107, 1976.
9. **Cooke, J. R., Rand, R. H., Mang, H. A., and DeBaerdemaeker, J. G.,** A nonlinear finite element analysis of stomatal guard cells, ASAE Paper No. 77-5511, American Society of Agricultural Engineers, St. Joseph, Mich., 1977.
10. **Cowan, I. R. and Milthorpe, F. L.,** Plant factors influencing the water status of plant tissues, in *Water Deficits and Plant Growth*, Vol. 1, Kozlowski, T. T., Ed., Academic Press, New York, 1968, 137.
11. **Dainty, J.,** Electrical analogues in biology, *Symp. Soc. Exp. Biol.*, 14, 140, 1960.
12. **Delwiche, M. J. and Cooke, J. R.,** An analytical model of the hydraulic aspects of stomatal dynamics, *J. Theor. Biol.*, 69, 113, 1977.
13. **deWit, C. T.,** Transpiration and crop yields, *Versl. Landbouwkd. Onderz*, 64(6), 1, 1958.
14. **El-Sharkawy, M. and Hesketh, J.,** Photosynthesis among species in relation to characteristics of leaf anatomy and CO_2 diffusion resistances, *Crop Sci.*, 5, 517, 1965.
15. **Gaastra, P.,** Photosynthesis of crop plants as influenced by light, carbon dioxide, temperature, and stomatal diffusion resistance, *Meded. Landbouwhogesch. Wageningen*, 59(13), 1, 1959.
16. **Gaastra, P.,** Climatic control in photosynthesis and respiration, in *Environmental Control of Plant Growth*, Evans, L. T., Ed., Academic Press, New York, 1963, 113.
17. **Gifford, R. M. and Musgrave, R. B.,** Stomatal role in the variability of net CO_2 exchange rates by two maize inbreds, *Aust. J. Biol. Sci.*, 26, 35, 1973.
18. **Holcomb, D. P. and Cooke, J. R.,** Diffusion resistance of porometer calibration plates determined with an electrolytic tank analog, ASAE Paper No. 77-5509, American Society of Agricultural Engineers, St. Joseph, Mich., 1977.
19. **Holcomb, D. P. and Cooke, J. R.,** An electrolytic tank analog determination of stomatal diffusion resistance, ASAE Paper No. 77-5510, American Society of Agricultural Engineers, St. Joseph, Mich., 1977.
20. **Holmgren, P., Jarvis, P. G., and Jarvis, M. S.,** Resistances to carbon dioxide and water vapour transfer in leaves of different plant species, *Physiol. Plant.*, 18, 557, 1965.
21. **Jarman, P. D.,** The diffusion of carbon dioxide and water vapour through stomata, *J. Exp. Bot.*, 25(88), 927, 1974.
22. **Jarvis, P. G.,** The estimation of resistances to carbon dioxide transfer, in *Plant Photosynthetic Production, Manual of Methods*, Sestak, A., Catsky, J., and Jarvis, P. G., Eds., Dr. W. Junk, N. V. Publishers, The Hague, 1971, 566.
23. **Jarvis, P. G. and Slatyer, R. O.,** The role of the mesophyll cell wall in leaf transpiration, *Planta (Berl.)*, 90, 303, 1970.
24. **Jones, H. G.,** Gas exchange in plant leaves having different transfer resistances through their two surfaces, *Aust. J. Biol. Sci.*, 26, 1045, 1973.
25. **Jones, H. G. and Slatyer, R. O.,** Effects of intercellular resistances on estimates of the intracellular resistance to CO_2 uptake by plant leaves, *Aust. J. Biol. Sci.*, 25, 443, 1972.
26. **Kramer, P. J.,** Transpiration and the water economy of plants, in *Plant Physiology, A Treatise*, Steward, F. C., Ed., Academic Press, New York, 1959, 607.
27. **Larmor, J.,** On transpiration through leaf-stomata, *Philos. Mag.*, 35, 350, 1918.

28. **Lee, R.,** The hydrologic importance of transpiration control by stomata, *Water Resour. Res.*, 3, 737, 1967.
29. **Lee, R. and Gates, D. M.,** Diffusion resistance in leaves as related to their stomatal anatomy and micro-structure, *Am. J. Bot.*, 51(9), 963, 1964.
30. **Livingston, B. E. and Brown, W. H.,** Relation of the daily march of transpiration to variations in the water content of foliage leaves, *Bot. Gaz. (Chicago)*, 53, 309, 1912.
31. **Maskell, E. J.,** Experimental researches on vegetable assimilation and respiration. XVIII. The relation between stomatal opening and assimilation. A critical study of assimilation rates and porometer rates in leaves of cherry laurel, *Proc. R. Soc. London, Ser. B.*, 102, 488, 1928.
32. **Meidner, H.,** Water supply, evaporation and vapour diffusion in leaves, *J. Exp. Bot.*, 26(94), 666, 1975.
33. **Meidner, H.,** Water vapour loss from a physical model of a substomatal cavity, *J. Exp. Bot.*, 27(99), 691, 1976.
34. **Meidner, H. and Mansfield, T. A.,** *Physiology of Stomata*, McGraw-Hill, New York, 1968.
35. **Merva, G. E.,** *Physioengineering Principles*, AVI Publishing, Westport, Conn., 1975.
36. **Milthorpe, F. L.,** Plant factors involved in transpiration, in *Plant Water Relationships, Arid Zone Research XVI*, United Nations Educational, Scientific, and Cultural Organization, Paris, 1961, 107.
37. **Monteith, J. L.,** Gas exchange in plant communities, in *Environmental Control of Plant Growth*, Evans, L. T., Ed., Academic Press, New York, 1963, 95.
38. **Monteith, J. L.,** *Principles of Environmental Physics*, American Elsevier, New York, 1973.
39. **Nobel, P. S.,** *Introduction to Biophysical Plant Physiology*, W. H. Freeman, San Francisco, 1974.
40. **Nobel, P. S.,** Effective thickness and resistance of the air boundary layer adjacent to spherical plant parts, *J. Exp. Bot.*, 26(90), 120, 1975.
41. **Nobel, P. S.,** Photosynthetic rates of sun versus shade leaves of *Hyptis emoryi*, Torr, *Plant Physiol.*, 58, 218, 1976.
42. **Nobel, P. S.,** Internal leaf area and cellular CO_2 resistance: photosynthetic implications of variations with growth conditions and plant species, *Plant Physiol.*, 40, 137, 1977.
43. **Nobel, P. S., Zaragoza, L. J., and Smith, W. K.,** Relation between mesophyll surface area, photosynthetic rate, and illumination level during development for leaves of *Plectranthus parviflorus* Henckel, *Plant Physiol.*, 55, 1067, 1975.
44. **Parkhurst, D. F.,** A three-dimensional model for CO_2 uptake by continuously distributed mesophyll in leaves, *J. Theor. Biol.*, 67, 471, 1977.
45. **Parlange, J. Y. and Waggoner, P. E.,** Stomatal dimensions and resistance to diffusion, *Plant Physiol.*, 46, 337, 1970.
46. **Penman, H. L. and Schofield, R. K.,** Some physical aspects of assimilation and transpiration, *Symp. Soc. Exp. Biol.*, 5, 115, 1951.
47. **Rand, R. H.,** Gaseous diffusion in the leaf interior, *Trans. ASAE*, 20(4), 701, 1977.
48. **Rand, R. H.,** Gaseous diffusion in the leaf interior, in *1977 Biomechanics Symposium*, Vol. 23, American Society of Mechanical Engineers, Applied Mechanics Division, New York, 1977, 51.
49. **Rand, R. H.,** A theoretical analysis of CO_2 absorption in sun versus shade leaves, *J. Biomechanical Engr., Trans. ASME*, 100, 20, 1978.
50. **Raschke, K.,** Stomatal action, *Annu. Rev. Plant Physiol.*, 26, 309, 1975.
51. **Renner, O.,** Beiträge zur Physik der Transpiration, *Flora*, 100, 451, 1910.
52. **Sinclair, T. R., Goudriaan, J., and deWit, C. T.,** Mesophyll resistance and CO_2 compensation concentration in leaf photosynthesis models, *Photosynthetica*, 11, 56, 1977.
53. **Sinclair, T. R. and Rand, R. H.,** Mathematical analysis of CO_2 assimilation under high CO_2 concentrations, *Photosynthetica*, 13(3), 1979, in press.
54. **Slatyer, R. O.,** Some physical aspects of internal control of leaf transpiration, *Agric. Meteorol.*, 3, 281, 1966.
55. **Slatyer, R. O.,** *Plant-Water Relationships*, Academic Press, New York, 1967.
56. **Tanton, T. W. and Crowdy, S. H.,** Water pathways in higher plants. III. The transpiration stream within leaves, *J. Exp. Bot.*, 23(76), 619, 1972.
57. **Tenhunen, J. D., Hesketh, J. D., and Gates, D. M.,** Leaf photosynthesis models, in *Predicting Photosynthesis for Ecosystem Models*, Vol. 1, Hesketh, J. D. and Jones, J. W., Eds., CRC Press, West Palm Beach, Fla., 1979, chap. 6.
58. **Thornley, J. H. M.,** *Mathematical Models in Plant Physiology*, Academic Press, New York, 1976.
59. **Ting, I. P. and Loomis, W. E.,** Diffusion through stomates, *Am. J. Bot.*, 50, 886, 1963.
60. **Ting, I. P. and Loomis, W. E.,** Further studies concerning stomatal diffusion, *Plant Physiol.*, 40, 220, 1965.
61. **Troughton, J. H. and Slatyer, R. O.,** Plant water status, leaf temperature, and the calculated mesophyll resistance to carbon dioxide of cotton leaves, *Aust. J. Biol. Sci.*, 22, 815, 1969.

62. **van den Honert, T. H.,** Water transport in plants as a catenary process, *Faraday Soc. Disc.*, 3, 146, 1948.
63. **Verduin, J.,** Diffusion through multiperforate septa, in *Photosynthesis in Plants*, American Society of Plant Physiologists, Bethesda, Md., 1947, 95.
64. **Waggoner, P. E.,** Relative effectiveness of change in upper and lower stomatal openings, *Crop Sci.*, 5, 291, 1965.
65. **Waggoner, P. E. and Zelitch, I.,** Transpiration and the stomata of leaves, *Science*, 150, 1413, 1965.